PRE-COLOMBIAN FUNERARY MASK VK_D_2256_462 - CU AS ALLOY - UNKNOWN - PERU

Artefact name Pre-Colombian funerary mask VK_D_2256_462

Authors (HE-Arc CR, Neuchâtel, Neuchâtel, Switzerland). (Christian Degrigny, None) & Valentin. Boissonnas (HE-Arc CR, Neuchâtel, Neuchâtel, Switzerland) & Audrey. Pera (HE-ARC CR, Neuchâtel, Neuchâtel, Switzerland)

Url /artefacts/1650/

The object



Fig. 1: Funeral mask, front side,

Credit HE-Arc CR, A.Pera.



Fig. 2: Funeral mask, rear side,

Credit HE-Arc CR, A.Pera.

Description and visual observation

This work is licensed under CC BY-NC-ND 4.0

Description of the artefact	This pre-Columbian funerary mask originates from the Chicama Valley in Peru. It is produced from a single sheet of metal. The nose is a separate piece, attached to the metal sheet by six staples. Blue-green and reddish-brown corrosion products are visible. The burial conditions caused the mask to corrode differently between the sides and the center (Fig. 3). There is a gap of a few centimeters in the upper right section, and a detached fragment—originally from the lower section—is associated with the mask (Fig. 5). Dimensions: Length = 30cm, Width = 19cm, Height = 4cm.
Type of artefact	Funeral mask
Origin	Chicama valley, Peru
Recovering date	None
Chronology category	Unknown
chronology tpq	----
chronology taq	----
Chronology comment	
Burial conditions / environment	Unknown
Artefact location	Kulturmuseum St-Gallen
Owner	Kulturmuseum St-Gallen
Inv. number	VK_D_2256_462
Recorded conservation data	N/A

Complementary information

By visual observation, we can see some beige fibres, the weave of a textile is printed on the corrosion products and some mineralised fibres are visible. An unknown substance is present on the eyes.

Study area(s)



Credit HE-ARC CR, A.Pera.

Fig. 3: The central part of the funeral mask is highlighted in green and sides parts in blue,

This work is licensed under CC BY-NC-ND 4.0



Fig. 4: Front side of the mask showing the location of individual samples analysed with SEM-EDS (A3 ; A4 ; A5 ; A6), FTIR (A3 ; A6) and of the sample analysed in cross-section with SEM-EDS (rectangle in black),

Credit HE-Arc CR, A.Pera.



Fig. 5: Detail of the fragment used for the cross-section,

Credit HE-Arc CR, A.Pera.

Binocular observation and representation of the corrosion structure

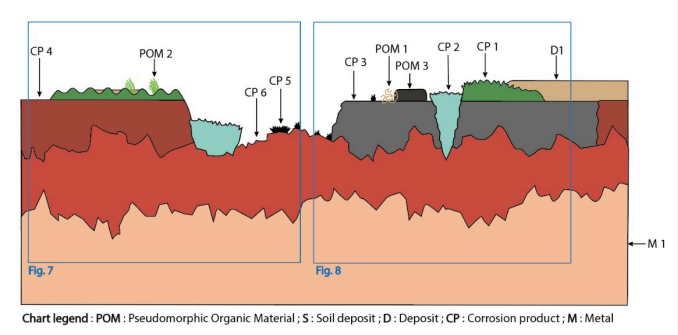
The schematic representation below gives an overview of the corrosion structures encountered on the funeral mask from a first visual macroscopic observation.

Strata	Type of strata	Principals characteristics
D1	Deposit	Layer, light brown, thin, discontinuous, matte, opaque, friable, soft
POM 1	Organic remains	Light brown, medium, isolated, non-observable brightness
POM2	Organic remains	Light green, thin, discontinuous, matte, opaque, brittle, soft
POM3	Organic remains	Layer, extra dark grey, medium, isolated, matte, opaque
CP1	Corrosion product	Layer, dark green, medium, discountinuous, matte, opaque, compact, severable, hard
CP2	Corrosion product	Lens-shaped, pale turquoise, medium, isolated, matte, opaque, powdery, very soft
CP3	Corrosion product	Layer, dark grey, thin, continuous, metallic, opaque, compact, malleable, soft
CP4	Corrosion product	Layer, dark red, thin, continuous, matte, opaque, friable, hard
CP5	Corrosion product	Veins or seams, black, thin, scattered, matt, opaque, non-compact, brittle, soft
CP6	Corrosion product	Layer, dark orange, thin, scattered, matte, opaque, compact, severable

This work is licensed under CC BY-NC-ND 4.0

M1	Metal	Layer, light orange, medium, continuous, metallic, opaque, compact, tough, hard

Table 1 : Description of the characteristics of the strata as observed under binocular.



Credit HE-ARC_A.Pera.

Fig. 6: Stratigraphic representation of the corrosion structures of the mask by binocular observation with indication of those used to build the MiCorr stratigraphies of Figs. 7 and 8 (blue squares),

MiCorr stratigraphy(ies) – Bi

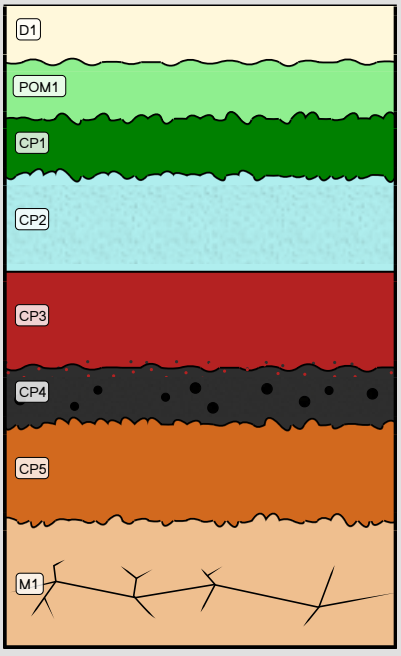


Fig. 7: Stratigraphic representation of the corrosion structure of the sides of the mask observed macroscopically under binocular microscope using the MiCorr application with reference to Fig. 6. The characteristics of the strata are only accessible by clicking on the drawing that redirects you to the search tool by stratigraphy representation. CP4, CP5, CP6 and POM2 on Fig. 6 are CP3, CP4, CP5 and POM1, credit HE-Arc CR, A.Pera.

This work is licensed under CC BY-NC-ND 4.0

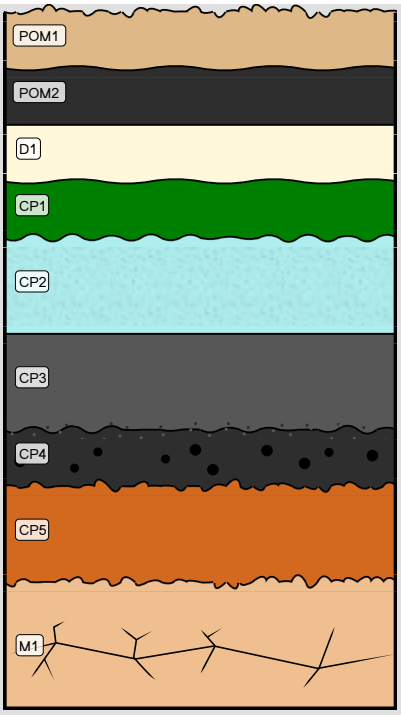
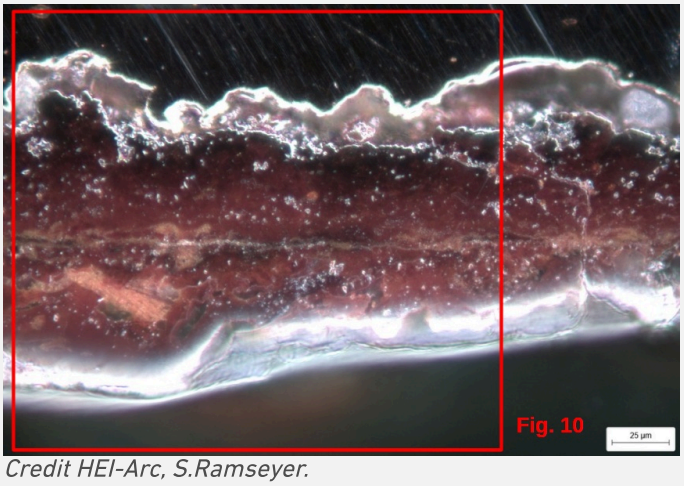


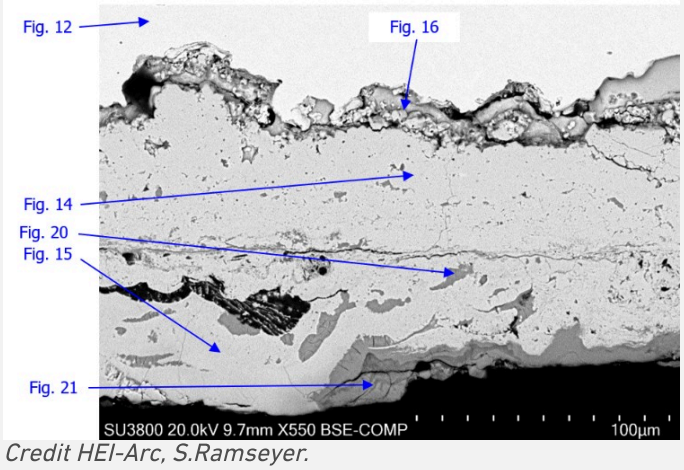
Fig. 8: Stratigraphic representation of the corrosion structure of the centre of the mask observed macroscopically under binocular microscope using the MiCorr application (C.f Fig. 6). The characteristics of the strata are only accessible by clicking on the drawing that redirects you to the search tool by stratigraphy representation. CP5, CP6 and POM3 on Fig. 6 are CP4, CP5 and POM 2, credit HE-Arc CR, A.Pera.

Sample(s)



Credit HEI-Arc, S.Ramseyer.

Fig. 9: Micrograph (detail, dark field) of the sample of the mask examined in cross section with location of Fig. 10,



Credit HEI-Arc, S.Ramseyer.

Fig. 10: SEM micrograph (detail) of the cross section of Fig. 9, with location of the following EDS analyses,

This work is licensed under CC BY-NC-ND 4.0

Description of sample	As illustrated on Figs. 4 and 5, the sample was taken on the detached fragment of the mask. The fragment shows a higher degree of mineralization than the rest of the mask (Fig. 11). It may have become detached during burial and been subjected to different burial conditions from the mask. Dimensions: 3x3mm.
Alloy	Cu As Alloy
Technology	Annealed after cold working
Lab number of sample	
Sample location	None
Responsible institution	None
Date and aim of sampling	Sampling aimed to study the composition, corrosion, and microstructural properties of the artefact.

Complementary information

It was temporarily embedded in a methyl methacrylate-based resin to examine its cross-section. After the resin was removed, the sample was reintegrated into the object.

Analyses and results

Analysis performed :

Non-invasive approach

- XRF, handheld device Thermo ScientificTM Nixton XL3t Goldd +, general metal mode (20s Main / 20s Low / 20 s Light) and mining mode (20s Main / 20s Lw / 20s High / 20s Light)
- X-radiography (59kV, 5 mA, 60s, d = 100cm)

Invasive approach

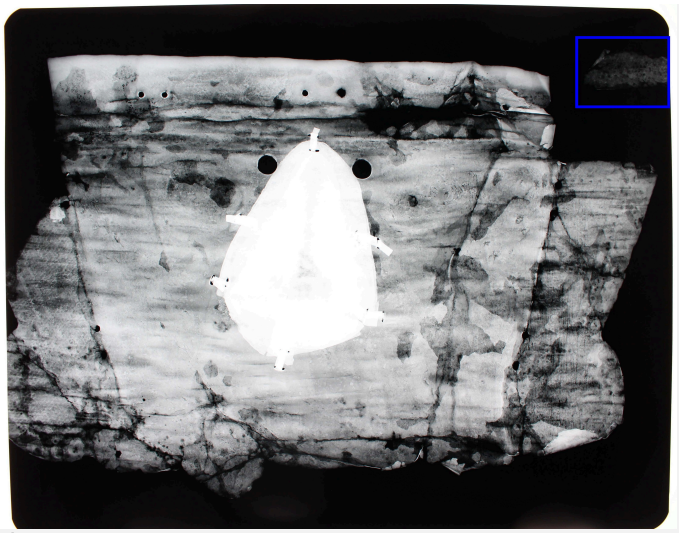
- SEM-EDS performed on individual samples and on the cross-section using a SEM-FEG JEOL 7001-F equipped with a silicon-drift EDS Oxford detector (Aztec analysis software) with an accelerating voltage of 20kV
- Metallography: the cross-section was observed before and after etching with aqueous chloride iron reagent
- FTIR spectroscopy using Thermo ScientificTM Nicolet iN10MX spectrometer and Thermo ScientificTM OMNIC software

Non invasive analysis

XRF performed directly on the metal surface of the mask with mining mode indicated the presence of arsenic (around 1% in mass).

X-ray radiography (Fig. 11) shows traces of hammering and embossed decorations on the ears. Gaps (top right) and areas of reduced density (top left and centre-right) appear darker. The metal at the nose appears denser, but this is due to the overlapping of sheets in that area. Because of its almost entirely mineralisation, the sample is barely discernible (blue rectangle).

This work is licensed under CC BY-NC-ND 4.0



Credit HKB, K.Wyss Heeb.

Fig.11: X-radiography of the mask. The detached fragment is inside the blue rectangle,

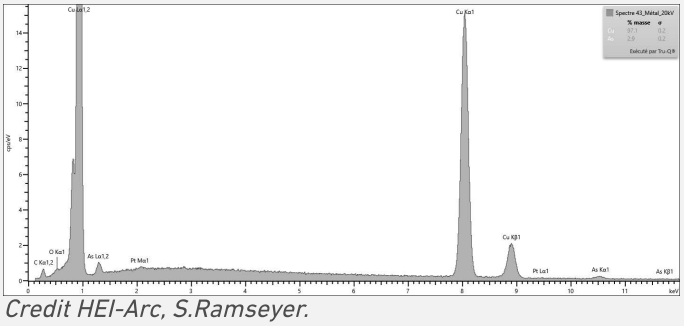
Metal

The metal analysed in cross-section with EDS consists of a copper-arsenic alloy (Fig. 12 and Table 2). It confirms the preliminary result obtained with XRF.

Elements	Cu	As
Mass %	97.1	2.9

Table 2: EDS analysis of the metal of the mask.

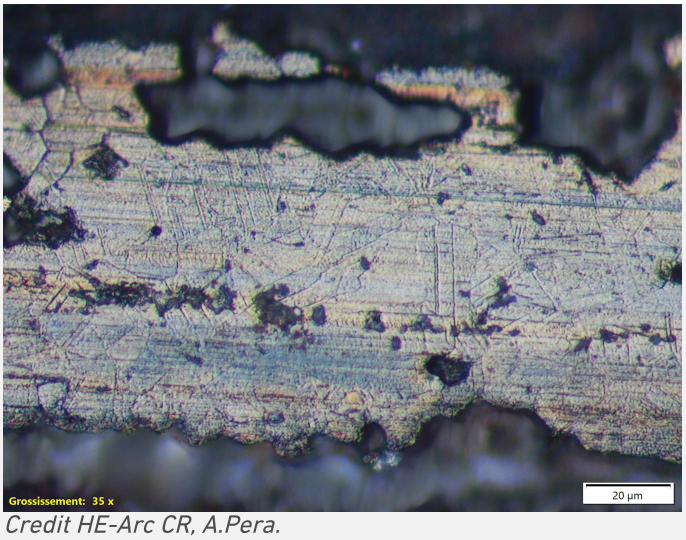
The microstructure of the metal shows some hexagonals grains with twinned lines which indicate that the metal sheet was annealed after cold-working (Scott, 1991) (Fig. 13).



Credit HEI-Arc, S.Ramseyer.

Fig. 12: EDS spectrum obtained in the metal core analysed on the cross-section in Fig. 10,

This work is licensed under CC BY-NC-ND 4.0



Credit HE-Arc CR, A.Pera.

Fig.13: Micrograph of the cross section etched and observed under metallographic microscope. Hexagonals grains with twinned lines are observed,

Microstructure	Large polygonal grains with few twins
First metal element	Cu
Other metal elements	As

Complementary information

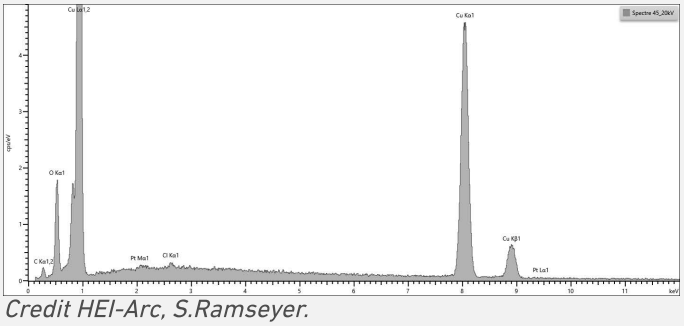
None.

Corrosion layers

The central part of the mask (Fig. 3) features a smooth, grey surface layer (CP3, Fig. 6). In places, across the entire mask, a smooth dark red layer (CP4, Fig 6) can be observed. On the nose and on the upper part of the mask a thick layer of green corrosion product (not analysed) is visible (CP1, Fig. 6). The sides of the mask (around the ears (Fig.3)) present a more irregular surface containing mineralized fibers (POM1, Fig. 6) on the same green corrosion layer (CP1, Fig. 6). Underneath a dark orange layer is present (CP6, Fig. 6) with black, powdery veins (CP5). Pale, powdery blue spots appear scattered (CP2).

The dark reddish-orange/brown layer (CP4 and CP6, Fig. 6), composed primarily of copper and oxygen, can be identified as cuprite (Figs. 14 and 15). EDS analysis performed at the interface between the remaining metal and the corrosion products reveals the presence of high concentration of chlorides (Fig. 16, nantokite?). FTIR analysis of two areas of powdery, light-blue corrosion products (CP2, Fig. 6) yielded results consistent with atacamite (Fig. 17), a copper hydroxychloride resulting from an active corrosion process.

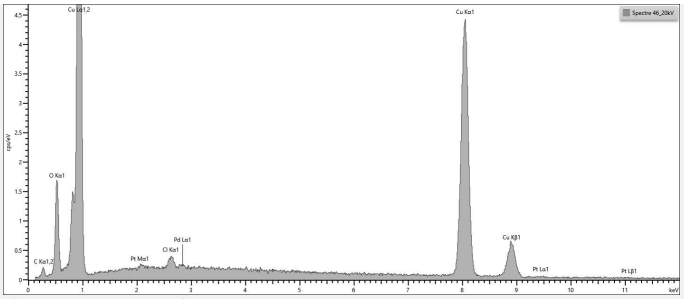
The object was likely exposed to a sulfur-rich environment, causing the appearance of black spots (Fig. 18). Other elements (Ca and Cl) have been identified on the top surface (Figs. 19 to 21).



Credit HEI-Arc, S.Ramseyer.

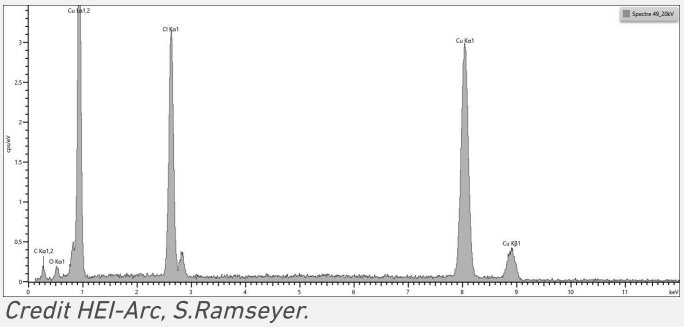
Fig. 14: EDS spectrum of light grey corrosion product in Fig. 10 (brown-reddish - CP6 in Fig. 9). The presence of Pt is attributed to the sample coating applied for SEM-EDS analysis,

This work is licensed under CC BY-NC-ND 4.0



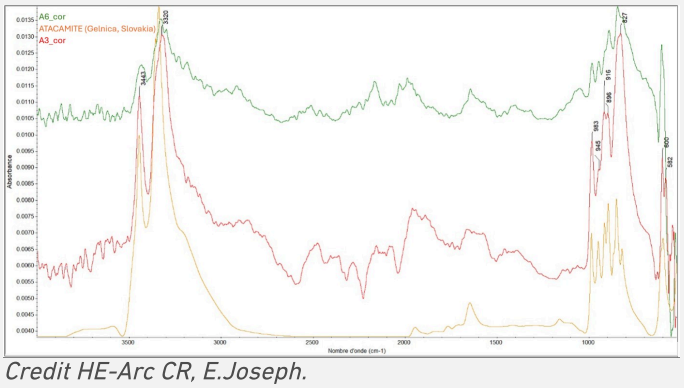
Credit HEI-Arc, S.Ramseyer.

Fig. 15: EDS spectrum of light grey corrosion product in Fig. 10 (brown-reddish - CP4 in Fig. 9). The presence of Pt and Pd is attributed to the sample coating applied for SEM-EDS analysis,



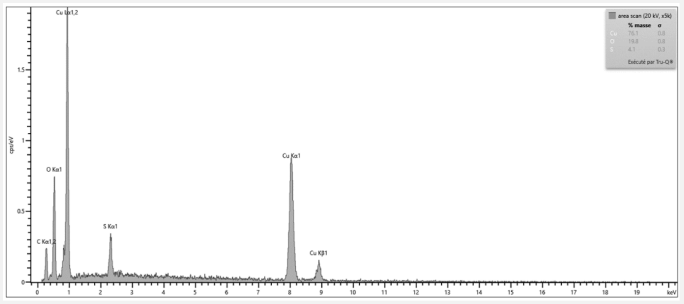
Credit HEI-Arc, S.Ramseyer.

Fig. 16: EDS spectrum at the interface between the remaining metal and the corrosion products in Fig. 10,



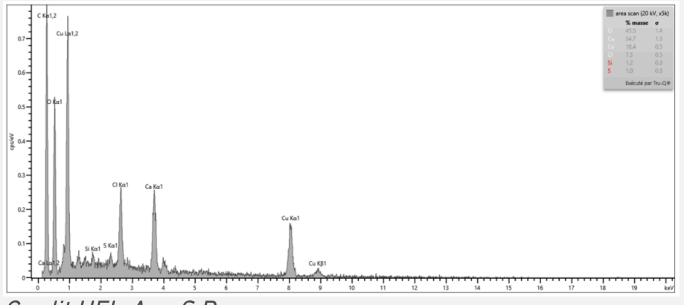
Credit HE-Arc CR, E.Joseph.

Fig.17: FTIR spectra realised on the A3 and A6 samples (Fig. 4) show a correlation with atacamite,



Credit HE-Arc CR, S.Ramseyer.

Fig. 18: EDS spectrum of the individual sample A4 (Fig. 4),



Credit HEI- Arc, S.Ramseyer.

Fig. 19: EDS spectrum of the individual sample A5 (Fig. 4),

This work is licensed under CC BY-NC-ND 4.0

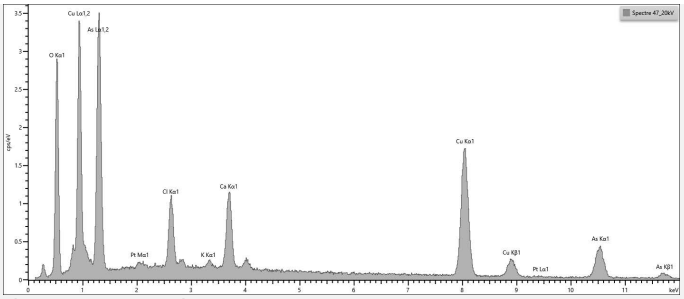


Fig. 20: EDS spectrum of the dark grey corrosion product in Fig. 10,

Credit HEI-Arc, S.Ramseyer.

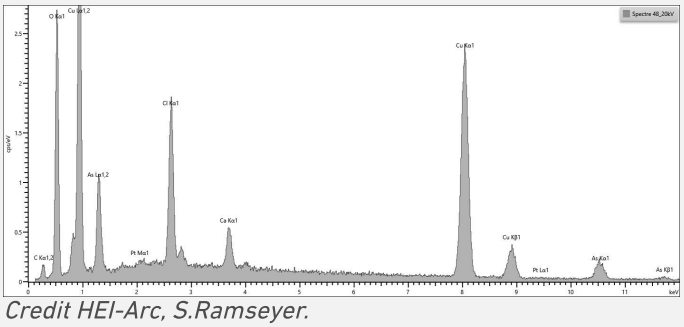


Fig. 21: EDS spectrum of the dark grey corrosion product in Fig. 10,

Credit HEI-Arc, S.Ramseyer.

Corrosion form Multiform

Corrosion type Mostly type I with locally type II (Robbiola)

Complementary information

None.

MiCorr stratigraphy(ies) – CS

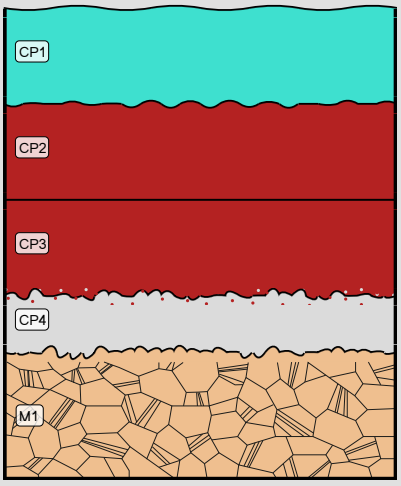


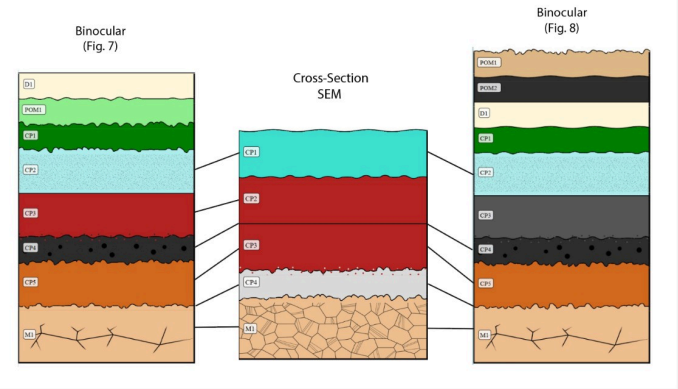
Fig. 22: Stratigraphic representation of the sample taken from the fragment of the funeral mask in cross-section under dark field using the MiCorr application. The characteristics of the strata are only accessible by clicking on the drawing that redirects you to the search tool by stratigraphy representation. This representation was built according to Fig. 9, Credit HE-Arc CR, A.Pera.

Synthesis of the binocular / cross-section examination of the corrosion structure

The stratigraphies obtained via observation under a binocular microscope and through cross-sectional analysis exhibit several differences. The sample examined in cross-section comes from a detached fragment—originally from the lower part of the mask. It appears to align with the observations made under the binocular microscope, revealing a smooth, dark-red surface layer (Fig. 7), while also displaying a specific CP4 that is rich in chlorides.

This work is licensed under CC BY-NC-ND 4.0

In cross-section, CP1, CP2, and CP5 appear similar to CP2, CP3, and CP5 as observed under a binocular microscope. D1, POM1–3, and CP4 do not appear in cross-section, either due to poor adhesion or because they are absent from the sampled area.



Credit HE-Arc, A.Pera.

Fig. 23: Stratigraphic representation side by side of binocular views and cross-section (dark field),

Conclusion

The mask is made of a copper-arsenic alloy. The metal sheet underwent annealing after work-hardening. A difference in corrosion products is observed between the edges of the mask and its central section: the center displays a smooth, grey layer and locally, across the entire surface, a smooth dark red layer whereas the edges reveal the imprint of a textile weave as well as mineralized fibers.

The reddish-orange/brown corrosion product was identified as cuprite. The presence of chlorides at the metal/corrosion-product interface prompted further investigation and an analysis of the light-blue, powdery spots found on the surface. These were identified as a hydroxychloride (such as atacamite). Consequently, a process of active corrosion may be underway.

References

References on object and analytical methods

Scott, D. 1991. ***Metallography and Microstructure of Ancient and Historic Metals.*** Marina del Rey, CA : Getty Conservation Institute in association with Archetype Books.

This work is licensed under CC BY-NC-ND 4.0